SINGLE PARTICLE DENSITY AND DENSITY MATRIX FROM THE QCD CASCADE IN DLA APPROXIMATION* **

B. Ziaja †

Institute of Physics, Jagellonian University
Reymonta 4, 30-059 Cracow, Poland
e-mail: beataz@thrisc.if.uj.edu.pl

(Received June 11, 1997)

The structure of the QCD gluonic cascade in configuration space is investigated. The explicit form of the inclusive single particle density in configuration space transverse coordinates is derived in the double logarithmic approximation (DLA) of QCD. The possible simplification of the multiparton density matrix formalism for DLA approach is found and discussed.

PACS numbers: 12.38. Aw, 12.38. Lg

1. Introduction

The aim of this talk is to present the recent results of the investigation [1] of the structure of the QCD gluonic cascade in configuration space. The interest of the configuration space structure of a hadronic source has appeared primarily in intensity interferometry [2]. The technique was developed originally to estimate the dimension of distant astronomical objects. Since that time it has seen widespread application in subatomic physics, in particular in analysis of elementary particle collisions [3]. The standard HBT procedure involves introducing an ansatz describing the geometry of the particle source, on the basis of a physical model. Then it investigates its multiparticle characterists in momentum space. Many models of hadron production based on some phenomenological or theoretical constraints [3]

---

* Presented at the XXXVII Cracow School of Theoretical Physics Zakopane, Poland, May 30–June 10, 1997.

** Work supported in part by the KBN grant: 2 PO 3B 08308 and by the European Human Capital and Mobility Program ERBCIPDCT940613.

† A fellow of the Foundation for the Polish Science '97.

have been considered; however, the question as to what is the configuration space structure of the QCD cascade when derived explicitly from the fundamental theory has not been addressed so far.

Recently, several groups have analysed in great detail the multiparton distributions in the QCD gluonic cascades [4]. The results of their investigations show that perturbative QCD [5] provides a powerful framework not only for the description of hard quark and gluon jets but also of much softer multiparticle phenomena. Although not understood theoretically, the hypothesis of parton-hadron duality [6] provides an apparently successful link between theoretical parton distributions and observed particle spectra. This prescription was extensively tested in single particle spectra (and total multiplicities) and found to be in a good agreement with the available data (see *e.g.* [7]). Recently, there have appeared indications that it may also work for multiparticle correlations [8]. These unquestionable successes invite one to study further consequences of the theory for processes of particle production. At this point we would like to notice that, if one wants to exploit fully the quantum-mechanical aspects of the QCD cascade, it is necessary to study at first the multiparton **density matrix**. The multiparticle distributions calculated so far give only diagonal terms of the density matrix and thus represent a rather restricted (although very important) part of the information available from the theory.

It is perhaps important to stress that in contrast to what is usually believed, the interest in studying the multiparticle density matrix is not purely academic. As suggested in [9], the density matrix allows one to obtain the multiparticle Wigner functions and consequently gives information about the space-time structure of the system. This allows one to make predictions about the shape and range of the HBT interference with clear experimental consequences.

In my previous paper [10] I investigated the multiparticle density matrix (DM) of the gluonic cascade produced in e^+e^- collision in the framework of double logarithmic (DLA) approximation [5], [11] of QCD. I proposed a generating functional to obtain integral equations for the multiparticle density matrix in the quasi-diagonal limit, *i.e.* if the energies and emission angles of particles are close to each other.

Here I will be presenting the technique for extracting physical information from the density matrix approach, deriving the explicit form of inclusive single particle density in configuration space. For the sake of simplicity, I will be restricting myself to a discussion of its dependence on the transverse space coordinate x_T. In solving the problem, first I will discuss the derivation of the inclusive single particle density matrix $d_P^{\rm in}(k',k)$. I will prove that the terms in $d_P^{\rm in}(k',k)$ which do not vanish for $k=k'$ are leading in the double logaritmic perturbative expansion when $\alpha_S \to 0$, momentum of quark (antiquark) P generating the gluonic cascade is large: $P \to \infty$ and the double logarithmic contributions of the form $\alpha_S \ln^2 P = const$ dominate. Taking into account these leading terms will allow me to obtain the explicit analytic form of the density matrix, and consequently the explicit form of the single particle density in configuration space. Finally, I will be analysing the physical properties of inclusive single particle density, and I hope to find them in agreement with intuitive physical expectations.

2. Density matrix formalism

2.1. Definition of the density matrix

In this paper I will concentrate on the single particle density in configuration space. I will be discussing it in relation to the QCD-parton cascade within the framework of double logarithmic approximation (DLA), using the density matrix formalism presented in [10]. Hence in this Section I will recall the definition of the density matrix for a particle production process, and show the relation between the density matrix and particle density in configuration space. Our assumption is that all the produced particles are real, *i.e.* they are on a mass shell. If the production of m particles can be realized in different ways represented by a sample of Feynman diagrams, then the exclusive m-particle density matrix equals the product of total production amplitude $S(k_1,..,k_m)$ and its complex conjugate $S^*(k'_1,..,k'_m)$ as:

$$d^{\rm ex}(k'_1,..,k'_m;k_1,..,k_m) = S^*(k'_1,..,k'_m)S(k_1,..,k_m)\,, \tag{1}$$

where the total amplitude $S(k_1,..,k_m)$ is the sum of all contributions $S_{(D)}$ from Feynman diagrams (D) multiplied by phase space factors $(2\omega_k)^{-1/2}$:

$$S(k_1,..,k_m) = \sum_D S_{(D)}(k_1,..,k_m)\prod_{i=1}^{m}(2\omega_{k_i})^{-1/2}. \tag{2}$$

For inclusive analysis one constructs the m-particle density matrix as a series of integrated n-particle exclusive densities in the form:

$$d^{\rm in}(\boldsymbol{k}'_1,..,\boldsymbol{k}'_m;\boldsymbol{k}_1,..,\boldsymbol{k}_m) = \sum_{n=m}^{\infty}\frac{1}{(n-m)!}\int [dk]_{m+1...n}\, d^{\rm ex}(\boldsymbol{k}'_1,..,\boldsymbol{k}'_m,\boldsymbol{k}_{m+1},..,\boldsymbol{k}_n;\boldsymbol{k}_1,..,\boldsymbol{k}_n), \tag{3}$$

where $[dk]_{i...j} \equiv d^3k_i..d^3k_j$. This construction scheme implies, that the diagonal elements of the density matrix are equal to particle densities in momentum space. There is also an obvious relation between the density matrix and particle density in real space. Remembering, that the space-time multiparticle amplitude is the on-mass-shell Fourier transform of the momentum amplitude, *i.e.*

$$S(x_1,...,x_m)=\int[dk]_{1...m}\,\mathrm{e}^{i\omega_{k_1}t_1-i\boldsymbol{k}_1\boldsymbol{x}_1}\,...\,\mathrm{e}^{i\omega_{k_m}t_m-i\boldsymbol{k}_m\boldsymbol{x}_m}\,S(k_1,...,k_m)\,,\quad(4)$$

where ω_{k_i} denotes the energy of the i-th produced particle, for the multiparticle density $\rho^{\mathrm{ex/in}}(x_1,...,x_m)$ we get the relation:

$$\begin{aligned}&\rho^{\mathrm{ex/in}}(x_1,...,x_m)\\&=\frac{1}{(2\pi)^{3m}}\int[dk]_{1...m}[dk']_{1...m}d^{\mathrm{ex/in}}(k_1',...,k_m';k_1,...,k_m)\\&\times\mathrm{e}^{i(\omega_{k_1}-\omega_{k_1'})t_1-i(\boldsymbol{k}_1-\boldsymbol{k}_1')\boldsymbol{x}_1}\,...\,\mathrm{e}^{i(\omega_{k_m}-\omega_{k_m'})t_m-i(\boldsymbol{k}_m-\boldsymbol{k}_m')\boldsymbol{x}_m}\,,\end{aligned}\quad(5)$$

where the factor $\frac{1}{(2\pi)^{3m}}$ was introduced to get the proper normalization:

$$\int[dx]_{1...m}\rho^{\mathrm{ex/in}}(x_1,...,x_m)=\int[dk]_{1...m}\rho^{\mathrm{ex/in}}(k_1,...,k_m).\quad(6)$$

2.2. Parton cascade in the double logarithmic approximation

The double logarithmic approach in momentum space [5,11] gives a good qualitative description of the structure of the gluonic cascade. It accounts only for the leading DL contributions to the multiparticle cross-section. Although emitted soft gluons violate the energy and momentum conservation rules, however, at high energies the approximation reproduces quite well the selfsimilar structure of the gluon radiation. Let us consider in the framework of DLA the gluonic cascade generated in e^+e^- collision. Multiparticle exclusive amplitude $S_{e_1...e_m}(k_1,...,k_m)$, describing the production of m gluons:

$$S_{e_1...e_m}(k_1,...,k_m)=(-1)^n\,\mathrm{e}^{-\frac{w(P)}{2}}\prod_{i=1}^{m}M_{P_i}(k_i)\,\mathrm{e}^{-\frac{w(k_i)}{2}}\,,\quad(7)$$

is a product of the m emission factors:

$$M_{P_i}(k_i)=g_S\frac{(e_i\cdot P_i)}{(k_i\cdot P_i)}\Theta_{P_i}(k_i)\,G_{P_i}\,,\quad(8)$$

where: $g_S=\sqrt{4\pi\alpha_s}$, n is the number of gluons emitted of quark (antiquark), $k_i=(\omega_i,\boldsymbol{k}_i)$ denotes the 4-momentum of the i-th soft gluon, $e_i\equiv e_i^{(j)}$, $j=0,...,3$ describes its polarization, P_i is the 4-momentum of the parent of the i-th gluon, G_{P_i} denotes the color factor for the given vertex of the tree diagram D, and can be conveniently represented as a tree diagram (see Fig. 1). Gluon emissions are not independent. Radiated particles have the memory of their parton parent, and of the previous parton splitting off its parent line. This dependence restricts the phase space of the produced gluon, and it is included in the form of a generalized step function $\Theta_{P_i}(k_i)$:

$$\Theta_P(k) := \{k^0 \equiv \omega < P^0,\, \theta_{kP} < \theta,\, \omega\theta_{kP} > Q_0\}\,, \tag{9}$$

where P is the momentum of the parent of a given parton k, θ denotes the emission angle of the previous parton splitting on the P–line, and Q_0 is a cut-off parameter. Virtual corrections appear as a radiation Sudakov factor $e^{-w(P)/2}$, where:

$$w(P) = \int d^3k\, \langle A_P^*(k) A_P(k)\rangle_{(e)} \tag{10}$$

denotes the total probability of emission of a gluon from the parent P, averaged over physical transverse polarizations ϵ^1, ϵ^2. $A_P(k)$ is given by:

$$A_P(k) = \frac{M_P(k)}{\sqrt{2\omega_k}}. \tag{11}$$

It should also be emphasized that produced gluons are real (on-mass-shell) particles, so the energy ω_k of a gluon of momentum k can be approximated as:

$$\omega_k = |\, \boldsymbol{k}\, |\,. \tag{12}$$

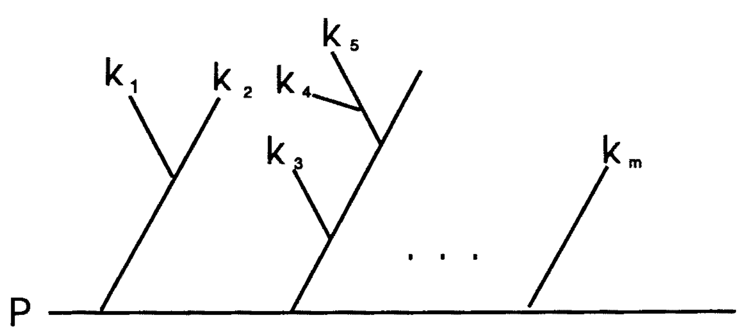

Fig. 1. Feynman diagram for the production of m gluons in DLA, where P denotes the 4-momentum of the initial $q(\bar{q})$ and k_i denotes the 4-momentum of the i-th produced gluon.

Summing of the color factors G over the color indices gives the result:

$$G_{P_i} G^*_{P_i} = \begin{cases} C_F \text{ for } P_i = P \\ C_V \text{ for } P_i \neq P\,, \end{cases} \tag{13}$$

where P denotes the 4-momentum of the quark (antiquark) which initializes the gluonic cascade.

In DLA different tree diagrams come from different non-overlapping kinematic regions, and do not interfere. Therefore, to calculate exclusive and inclusive multigluon densities it is enough to sum up incoherently the squares of amplitudes (7). Hence one obtains the exclusive density $\rho_P^{\mathrm{ex}}(\boldsymbol{k}_1, .., \boldsymbol{k}_m)$ in the form:

$$\rho_P^{\mathrm{ex}}(\boldsymbol{k}_1, .., \boldsymbol{k}_m) = \mathrm{e}^{-w(P)} \sum_D \prod_{i=1}^{m} \langle A^*_{P_i}(k_i) A_{P_i}(k_i)\rangle_{(e_i)}\, \mathrm{e}^{-w(k_i)} \tag{14}$$

parametrized by the momentum P of the quark (antiquark) which initializes the cascade. Multigluon inclusive density $\rho_P^{\mathrm{in}}(\boldsymbol{k}_1, .., \boldsymbol{k}_m)$ follows from (3) as:

$$\rho_P^{\mathrm{in}}(\boldsymbol{k}_1, .., \boldsymbol{k}_m) = \sum_{n=m}^{\infty} \frac{1}{(n-m)!} \int [dk]_{m+1...n}\, \rho_P^{\mathrm{ex}}(\boldsymbol{k}_1, .., \boldsymbol{k}_n). \tag{15}$$

Introducing the method of the generating functional (GF) (see [5] and references therein) allows us to perform the summation over diagrams in (14) and (15) in a very convenient way. While constructing the generating functional $Z_P[u]$, one applies explicitly the selfsimilarity property of the gluonic cascade. As a final result one obtains the recursive *master equation* in the form:

$$Z_P[u] = \mathrm{e}^{-w(P)} \exp\left(\int d^3k\, \langle A^*_P(k) A_P(k)\rangle_{(e)}\, u(k) Z_k[u] \right). \tag{16}$$

It can be proved [5] that equation (16) reproduces contributions of all tree diagrams D, and allows us to express multigluon densities $\rho_P^{\mathrm{in}}(\boldsymbol{k}_1, .., \boldsymbol{k}_m)$ and $\rho_P^{\mathrm{ex}}(\boldsymbol{k}_1, .., \boldsymbol{k}_m)$ as:

$$\rho_P^{\mathrm{ex}}(\boldsymbol{k}_1, .., \boldsymbol{k}_m) = \frac{\delta^m}{\delta u_1 ... \delta u_m} Z_P \,|_{\{u=0\}}\,, \tag{17}$$

$$\rho_P^{\mathrm{in}}(\boldsymbol{k}_1, .., \boldsymbol{k}_m) = \frac{\delta^m}{\delta u_1 ... \delta u_m} Z_P \,|_{\{u=1\}}\,, \tag{18}$$

where u_i denotes the probing function $u(k_i)$ and the functional derivative $\delta/\delta u_i$ denotes $\delta/\delta u(k_i)$ respectively.

We would like to emphasize the simplicity of the GF approach. Especially for inclusive densities the method allows us to skip the complicated summation procedure, and to express the required distribution in a simple, compact form (for details see [12]).

2.3. Density matrix in the DLA formalism

The DLA formalism in momentum space gives a good description of the structure of the gluonic cascade. The GF scheme suggests clearly how to construct multigluon densities, and allows us to investigate their properties in a simple way. Since the method works so well for multiparticle distributions, one can expect to apply it successfully for other multiparticle observables. Below we briefly discuss the calculation of the multiparticle density matrix in the framework of double logarithmic approximation, recalling our main results from Ref. [10].

First we derive the general expression for the exclusive and inclusive density matrices $d_P^{\rm ex}(\boldsymbol{k}'_1,..,\boldsymbol{k}'_m;\boldsymbol{k}_1,..,\boldsymbol{k}_m)$ and $d_P^{\rm in}(\boldsymbol{k}'_1,..,\boldsymbol{k}'_m;\boldsymbol{k}_1,..,\boldsymbol{k}_m)$. The task looks quite complicated because in this case the interference between different diagrams in (1), generally does not vanish. Let us define two functionals, $Z_P[u]$ and $Z^*_{P'}[w]$, which generate the sum of all tree amplitudes and the sum of their complex conjugates respectively:

$$
\begin{aligned}
Z_P[u] &= {\rm e}^{-w(P)/2}\exp\left(\int d^3k A_P(k)u(k)Z_k[u]\right),\\
Z^*_{P'}[s] &= {\rm e}^{-w(P')/2}\exp\left(\int d^3k A^*_{P'}(k)s(k)Z^*_k[s]\right). \qquad (19)
\end{aligned}
$$

The multigluon density matrices can be then expressed as (see Appendix A):

$$
\begin{aligned}
& d_P^{\rm ex}(\boldsymbol{k}'_1,..,\boldsymbol{k}'_m;\boldsymbol{k}_1,..,\boldsymbol{k}_m)\\
&= \frac{\delta^m}{\delta s_{1'}...\delta s_{m'}}\frac{\delta^m}{\delta u_1...\delta u_m} Z_P[u]Z^*_{P'}[s]\mid_{\{u=s=0\},P=P'}, \qquad (20)\\
& d_P^{\rm in}(\boldsymbol{k}'_1,..,\boldsymbol{k}'_m;\boldsymbol{k}_1,..,\boldsymbol{k}_m)\\
&= \frac{\delta^m}{\delta s_{1'}...\delta s_{m'}}\frac{\delta^m}{\delta u_1...\delta u_m} Z_P[u]Z^*_{P'}[s]\mid_{\{u=\frac{\delta}{\delta s},s=0\},P=P'}. \qquad (21)
\end{aligned}
$$

Eq. (21) is, in fact, a complicated integral equation. The difficulty of the diagram summation does not disappear there. It is only hidden in the compact form of (21). However, we remember that in the above formula we have taken into account interference between *all* different graphs D and D'. And detailed analysis gives the result that in DLA not all the diagrams mix up: one can distinguish some interference classes. However, at the general level we did not succeed in formulation of such a GF which would take this fact into account.

Nevertheless, we do not need the most general form of the density matrix. We are interested in its behaviour when the differences of momenta $\mid k_1-k'_1\mid,...,\mid k_m-k'_m\mid$ are small, since we expect that large momentum differences will not contribute to Fourier transforms [13]. It can be shown that

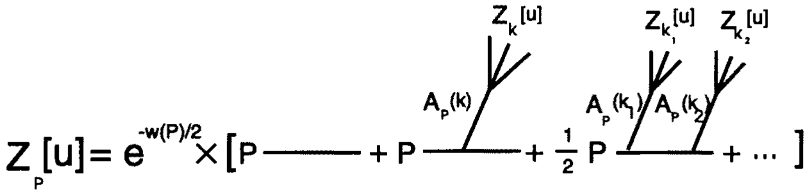

Fig. 2. Generating functional (19) as a diagram series.

within this limit interferences between different diagrams vanish, and one sums up only "squared" contributions from identical graphs. In fact, from the analysis of the diagrams contributing to single particle density matrix $d_P^{\rm ex}(k_1', k_1)$, it has been possible to prove (see Appendix B) that interference between different diagrams appears only if either energies or emission angles of produced particles are strongly ordered: $\omega_1 \gg \omega_{1'}$ ($\omega_1 \ll \omega_{1'}$) or $\theta_{1P} \gg \theta_{1'P}$ ($\theta_{1P} \ll \theta_{1'P}$). This statement can be generalized for any m-particle density matrix. If we have m particles, and $(m-1)$ ones among them are "close" to each other, *e.g.* $k_1 \cong k_1', \ldots, k_{m-1} \cong k_{m-1}'$, then the interference of the different diagrams will take place only if either the energies or the angles of k_m and k_m' are strongly ordered.

Hence in our approximation we exclude mixing up different diagrams, and sum up only the squared contributions from identical ones. The exclusive and inclusive density matrices then take the simpler form:

$$d_P^{\rm ex}(\boldsymbol{k}_1', \ldots, \boldsymbol{k}_m'; \boldsymbol{k}_1, \ldots, \boldsymbol{k}_m) = \sum_D \prod_{i=1}^m (4\omega_{k_i'}\omega_{k_i})^{-1/2} \langle S_{e_1 \ldots e_m}(k_1', \ldots, k_m') S_{e_1 \ldots e_m}(k_1, \ldots, k_m)\rangle_{(e_1 \ldots e_m)}, \quad (22)$$

$$d_P^{\rm in}(\boldsymbol{k}_1', \ldots, \boldsymbol{k}_m'; \boldsymbol{k}_1, \ldots, \boldsymbol{k}_m) = \sum_{n=m}^{\infty} \frac{1}{(n-m)!} \sum_D \int [dk]_{m+1 \ldots n} \prod_{i=1}^m (4\omega_{k_i'}\omega_{k_i})^{-1/2} \prod_{j=m+1}^n (4\omega_{k_j}\omega_{k_j})^{-1/2}$$
$$\times \langle S_{e_1 \ldots e_n}(k_1', \ldots, k_m', k_{m+1}, \ldots, k_n) S_{e_1 \ldots e_n}(k_1, \ldots, k_n)\rangle_{(e_1 \ldots e_n)}. \quad (23)$$

The summation in (23), (23) over D can be easily performed using the generating functional which reproduces only contributions of identical tree diagrams. In [10] I proposed a master equation for such a generating functional (GF) $Z_{P'P}[u(k', k)]$. It accounts only for the contributions of "diago-

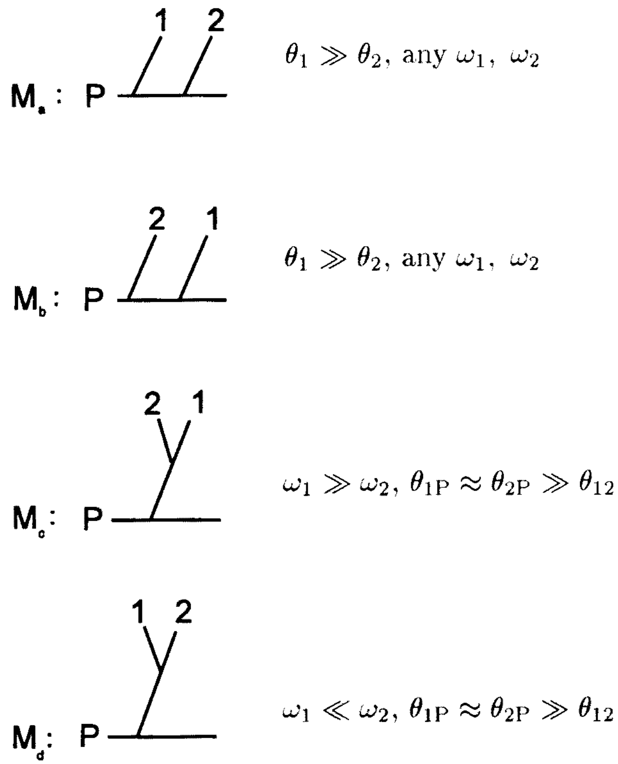

Fig. 3. Redefined kinematical regions in DLA.

nal" diagrams (for proof see Appendix C), and generates the exclusive and inclusive density matrix as:

$$d_P^{\rm ex}(\boldsymbol{k}'_1,..,\boldsymbol{k}'_m;\boldsymbol{k}_1,..,\boldsymbol{k}_m) = \frac{\delta^m}{\delta u_{m',m}..\delta u_{1',1}} Z_{P'P}\,|_{\{u=0\},P=P'}, \tag{24}$$

$$d_P^{\rm in}(\boldsymbol{k}'_1,..,\boldsymbol{k}'_m;\boldsymbol{k}_1,..,\boldsymbol{k}_m) = \frac{\delta^m}{\delta u_{m',m}..\delta u_{1',1}} Z_{P'P}\,|_{\{u=\delta^3(l'-l)\},P=P'}\,. \tag{25}$$

The explicit form of its master equation, and the other formulae needed for further calculations are presented below. The GF reads:

$$\begin{aligned} Z_{P'P}[u] \;=\; & \mathrm{e}^{-W(P',P)} \sum_{n=0}^{\infty} \frac{1}{n!} \int [dk']_{1...n}\,[dk]_{1...n}\, u(k'_1,k_1)...u(k'_n,k_n) \\ & \times \langle A^*_{P'}(k'_1) A_P(k_1)\rangle_{(\epsilon_1)} ... \langle A^*_{P'}(k'_n) A_P(k_n)\rangle_{(\epsilon_n)} \\ & \times Z_{k'_1 k_1}[u] ... Z_{k'_n k_n}[u]\, P_{1',...,n';1,...,n}\,, \end{aligned} \tag{26}$$

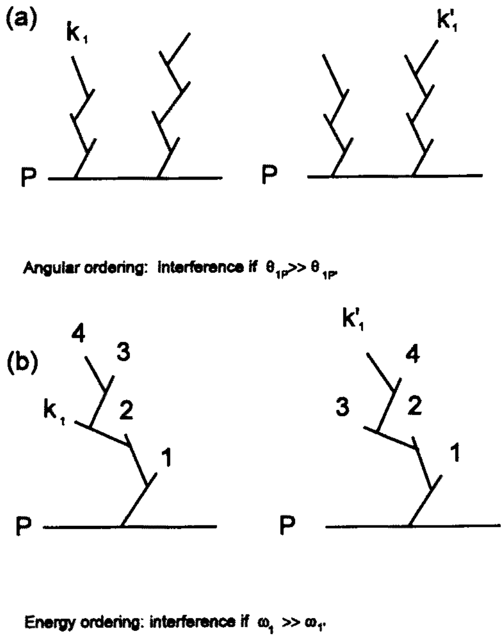

Fig. 4. Interference between different diagrams for $d_P^{\rm ex}(k_1', k_1)$. Remark: pairs of diagrams (a) and (b) are identical except of the position of k_1 (k_1') leg.

where the function $P_{1',\dots,n';1,\dots,n}$ provides the requested parallel angular ordering (see Fig. 5) for n particles in the form:

$$P_{1',\dots,n';1,\dots,n} = \sum_{(i_1,\dots,i_n)\in \mathrm{perm}(1,\dots,n)} \Theta(\theta_{k'_{i_1}P'} > \dots > \theta_{k'_{i_n}P'})\; \Theta(\theta_{k_{i_1}P} > \dots > \theta_{k_{i_n}P}) \tag{27}$$

the product of the single particle amplitudes $\langle\, A^*_{P'}(k')A_P(k)\rangle_{(e)}$ averaged over gluon polarizations (see Appendix D) reads:

$$\begin{aligned} &\langle A^*_{P'}(k')A_P(k)\rangle_{(e)} \equiv A_{P'P}(k',k) \\ &= \frac{4g_S^2}{2\pi}\, G^*_{P'}G_P\, \frac{1}{\sqrt{4\omega'^3\omega^3}}\, \frac{1}{\theta_{Pk}\theta_{P'k'}} \Theta_{P'}(k')\Theta_P(k); \end{aligned} \tag{28}$$

and the radiation factor is given by:

$$W(P',P) = \frac{w(P') + w(P)}{2}. \tag{29}$$

The other notations are the same as in Section 2. 2.

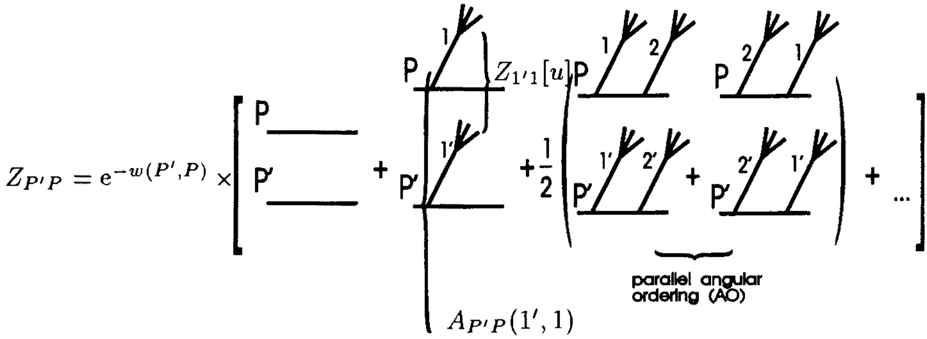

Fig. 5. Master equation for generating functional (26) represented as a diagram series (for details see [10]). Function $P_{1',\ldots,n';1,\ldots,n}$ introduces the parallel angular ordering (AO).

Generating functional (26) describes the sequence of "emissions": $\langle A^*_{P'}(k')A_P(k)\rangle_{(e)}$ of two particles k, k' from two parents P, P'. If the profile function $u(l', l)$ is equal to 0 and $\delta^3(l' - l)$ respectively, then the functional $Z_{P'P}$ takes the form:

$$\begin{aligned} Z_{P'P}[u = 0] &= e^{-W(P',P)}, \\ Z_{PP}[u = \delta^3(l' - l)] &= 1. \end{aligned} \tag{30}$$

For the profile function of the form $u(l', l) = v(l)\,\delta^3(l' - l)$ and $P = P'$ our $Z_{P'P}[u]$ reduces to functional (16), as expected:

$$Z_{PP}[u(l', l) = v(l)\,\delta^3(l' - l)] = Z_P[v(l)]. \tag{31}$$

2.4. Single particle density matrix. Leading terms

From relations (25), (26) one obtains a simple integral equation for the inclusive single particle density matrix:

$$\begin{aligned} d_P^{\text{in}}(k'; k) &= \int d^3 s A_{PP}(s, s) d_s^{\text{in}}(k'; k) \\ &\quad + f_P(k', k) A_{PP}(k', k)\, Z_{k',k}[u = \delta^3(l' - l)], \end{aligned} \tag{32}$$

where $f_P(k', k)$ equals

$$f_P(k', k) = e^{-g_S^2 C_F |\ln^2 \frac{\theta_{kP}P}{Q_0} - \ln^2 \frac{\theta_{k'P}P}{Q_0}|}. \tag{33}$$

Introducing the notation:

$$g_P(k',k) \equiv f_P(k',k)\, A_{PP}(k',k)\, Z_{k',k}[u = \delta^3(l'-l)] \tag{34}$$

we may write the symbolical solution $d_P^{\rm in}(k',k)$ of (32) in the form:

$$d_P^{\rm in}(k',k) = \sum_{n=0}^{\infty} \int d^3s_1 ... d^3s_n\, A_{PP}(s_1,s_1) ... A_{s_{n-1}s_{n-1}}(s_n,s_n) g_{s_n}(k',k). \tag{35}$$

We present Eq. (35) as a final result obtained in Ref. [10]. The exact solution of $d_P^{\rm in}(k',k)$ and its detailed properties will be discussed below. We may replace $A_{PP}(s,s)$ in (35) with its explicit form taken from Eq. (28):

$$\begin{aligned} d_P^{\rm in}(k',k) &= \sum_{n=0}^{\infty}(2b)^n \int \frac{ds_1}{s_1} \int \frac{d\Omega_{s_1}}{2\pi\theta_{Ps1}^2} \Theta_P(s_1) ... \int \frac{ds_n}{s_n} \int \frac{d\Omega_{s_n}}{2\pi\theta_{n-1,n}^2} \Theta_{s_{n-1}}(s_n) \\ &\quad \times g_{s_n}(k',k)\,, \end{aligned} \tag{36}$$

where $\int d\Omega_{s_i}$ denotes the angular integration over the direction of vector $\boldsymbol{s_i}$, $\Theta_{i,j} \equiv \Theta_{s_i,s_j}$ and $b \equiv g_S^2 C_F$. Factor $g_s(k',k)$ defined by expression (34), reads:

$$\begin{aligned} g_S(k',k) &= \frac{2b}{2\pi} \frac{1}{\sqrt{k^3k'^3}} \frac{1}{\theta_{Sk}\theta_{Sk'}} \Theta_S(k')\Theta_S(k) \\ &\quad \times \exp\left(-b \mid \ln^2 \frac{\theta_{kS}S}{Q_0} - \ln^2 \frac{\theta_{k'S}S}{Q_0} \mid\right) \\ &\quad \times \exp\left(-b'/2 \left(\ln^2 \frac{k\theta_{kS}}{Q_0} + \ln^2 \frac{k'\theta_{k'S}}{Q_0}\right)\right) \\ &\quad \times \sum_{n=0}^{\infty} (2b')^n \int [dk]_{1...n} \frac{1}{2\pi\theta_{k1}\theta_{k'1}} \cdots \frac{1}{2\pi\theta_{kn}\theta_{k'n}} \frac{1}{k_1^3} \cdots \frac{1}{k_n^3} \\ &\quad \times \Theta(\theta_{k1} > ... > \theta_{kn}) \Theta(\theta_{k'1} > ... > \theta_{k'n}) \\ &\quad \times \Theta_{k'}(1) . . \Theta_{k'}(n) \Theta_k(1) . . \Theta_k(n)\,, \end{aligned} \tag{37}$$

where $b' \equiv g_S^2 C_V$. Rewriting its phase space restrictions in terms of Bessel functions (see Appendix E) one arrives at:

$$\begin{aligned} g_S(k',k) &= \frac{2b}{2\pi} \frac{1}{\sqrt{k^3k'^3}} \frac{1}{\theta_{Sk}\theta_{Sk'}} \Theta_S(k')\Theta_S(k) \\ &\quad \times \exp\left(-b \mid \ln^2 \frac{\theta_{kS}S}{Q_0} - \ln^2 \frac{\theta_{k'S}S}{Q_0} \mid\right) \\ &\quad \times \exp\left(-b'/2 \left(\ln^2 \frac{k\theta_{kS}}{Q_0} + \ln^2 \frac{k'\theta_{k'S}}{Q_0}\right)\right) \end{aligned}$$

$$\times \sum_{n=0}^{\infty} (2b')^n \prod_{i=1}^{n} \left(\int_0^{\infty} dx_i x_i J_0(x_i \theta_{k'k}) \int_{\max\left(\frac{Q_0}{\theta_{k,i-1}}, \frac{Q_0}{\theta_{k',i-1}}\right)}^{\min(k,k')} \frac{dk_i}{k_i} \right.$$

$$\left. \times \int_{\frac{Q_0}{k_i}}^{\theta_{k,i-1}} d\theta_{ki} J_0(x_i \theta_{ki}) \int_{\frac{Q_0}{k_i}}^{\theta_{k',i-1}} d\theta_{k'i} J_0\left(x_i \theta_{k'i}\right) \right). \tag{38}$$

The term which dominates in (37) in the double logarithmic perturbative expansion: $b \to 0$, $P \to \infty$, $b \ln^2 \frac{P}{Q_0} = const$, has the explicit form (for details see Appendix F):

$$g_S^{(1)}(k', k) = \frac{2b}{2\pi} \frac{1}{\sqrt{k^3 k'^3}} \frac{1}{\theta_{Sk'} \theta_{Sk}} \Theta_S(k') \, \Theta_S(k). \tag{39}$$

One may check (see Appendix F) that this term iterated in (36) produces the DLA leading contribution to the density matrix $d_P^{\rm in}(k', k)$. Namely, if we introduce the notation:

$$d_P^{in,(1)}(k', k)$$
$$\equiv \sum_{n=0}^{\infty} (2b)^n \int \frac{ds_1}{s_1} \int \frac{d\Omega_{s_1}}{2\pi \theta_{P1}^2} \Theta_P(s_1) ... \int \frac{ds_n}{s_n} \int \frac{d\Omega_{s_n}}{2\pi \theta_{n-1,n}^2} \Theta_{s_{n-1}}(s_n)$$
$$\times g_{s_n}^{(1)}(k', k) \tag{40}$$

then there is a relation:

$$d_P^{\rm in}(k', k) \leq d_P^{\rm in,(1)}(k', k) \tag{41}$$

and for $k \cong k'$ in quasi-diagonal limit:

$$d_P^{\rm in}(k', k) \cong d_P^{\rm in,(1)}(k', k). \tag{42}$$

Both (41) and (42) hold in the perturbative limit, as well. Hence we may write finally that:

$$d_P^{\rm in}(k', k) \stackrel{\rm DLA}{=} \sum_{n=0}^{\infty} (2b)^n \int \frac{ds_1}{s_1} \int \frac{d\Omega_{s_1}}{2\pi \theta_{P1}^2} \Theta_P(s_1) ... \int \frac{ds_n}{s_n} \int \frac{d\Omega_{s_n}}{2\pi \theta_{n-1,n}^2} \Theta_{s_{n-1}}(s_n)$$
$$\times g_{s_n}^{(1)}(k', k). \tag{43}$$

The above result simplifies significantly the single particle density matrix approach [10]. We apply it in Section 4. 2. so as to improve calculation of the single particle density in mixed coordinates.

3. DLA in configuration space

3.1. Fourier transform in transverse coordinates

The DLA soft parton cascade starts from the initial parton of momentum $\boldsymbol{P}$. Momenta of all particles produced from parton P refer to the $\boldsymbol{P}$ direction: they depend on the **transverse and longitudinal** momenta $\boldsymbol{k}_{\rm T}$ and $k_{\rm L}$ (see *e.g.* [5, 14]) taken with respect to the $\boldsymbol{P}$ axis.

This dependence influences the structure of the cascade in configuration space. For the single particle amplitude Eq. (4) takes the form:

$$S_P(x) = \int d^3k \, e^{i\omega t - i\boldsymbol{k}\boldsymbol{x}} S_P(\boldsymbol{k}) = \int dk_{\rm L} d^2k_{\rm T} \, e^{i\omega t - i\boldsymbol{k}\boldsymbol{x}} \, S_P(\boldsymbol{k}) \,, \tag{44}$$

where $S_P(\boldsymbol{k})$ ($S_P(x)$) denotes the amplitude to produce a single particle with the momentum $\boldsymbol{k}$ (at the space-time coordinate x) from the initial particle of momentum $\boldsymbol{P}$, and the 3-dimensional product $\boldsymbol{k}\boldsymbol{x}$ reads:

$$\boldsymbol{k}\boldsymbol{x} = k_{\rm L}\, x_{\rm L} + \boldsymbol{k}_{\rm T}\, \boldsymbol{x}_{\rm T} \,, \tag{45}$$

where indices L and T denote longitudinal and transverse components of momenta and coordinates with respect to the $\boldsymbol{P}$ axis.

Since DLA amplitude $S_P = S_P(\omega, \theta_{Pk})$ (7) depends explicitly on $\omega =\mid \boldsymbol{k} \mid \equiv k$ (12) and θ_{Pk}, one should express it as a function of $k_{\rm L}$ and $\boldsymbol{k}_{\rm T}$. To proceed, let us recall that the simple form of $S_P = S_P(k, \theta_{Pk})$ has been obtained from the original QCD expression using the approximation of small emission angles $\theta_{Pk} \ll 1$ [5]. In this approximation one retains only the leading term in θ_{Pk}. Hence, restricting ourselves to the leading terms in θ_{Pk}, we interprete product $k\theta_{Pk}$ as the transverse momentum $k_{\rm T}$ and k as the longitudinal momentum $k_{\rm L}$. The correctness of the substitution $k \approx k_{\rm L}$ for e^{ikt} in (44) is not so evident, since it should be done in the argument of Fourier transform. However, if we restrict ourselves to finite, small time intervals, *i.e.* $t \ll (P\theta^2)^{-1}$, it also works with a high level of accuracy. To see this, let us analyse the dependence of k on $k_{\rm L}$ and $k_{\rm T}$. Following (12), it can be expressed as:

$$(\omega \equiv) k = \sqrt{k_{\rm L}^2 + k_{\rm T}^2}. \tag{46}$$

For intrajet cascades there is a relation $k_{\rm T} \ll k_{\rm L}$. Restricting ourselves to the leading term $k \approx k_{\rm L}$, we ignore the contributions of the order of $k_{\rm T}^2/k_{\rm L}$. In DLA the ratio $k_{\rm T}^2/k_{\rm L}^2$ has a limiting maximum value θ^2 denoting the emission angle of the previous parton splitting off the P-line (compare (9)). Maximal energy carried by the gluon equals P. Since that the approximation $k \approx k_{\rm L}$ implies, that one neglects terms of the order of $P\theta^2$.

Using the leading term approximation, Eq. (44) can be rewritten as the product of 2 separate Fourier transforms: 1-dimensional FT of $(k_{\rm L}, t - x_{\rm L})$, and 2-dimensional FT of $(\boldsymbol{k}_{\rm T}, -\boldsymbol{x}_{\rm T})$ in the form:

$$S_P(x_{\rm L}, \boldsymbol{x}_{\rm T}, t) = \int dk_{\rm L}\, {\rm e}^{ik_{\rm L}(t-x_{\rm L})} \int d^2k_{\rm T}\, {\rm e}^{-i\boldsymbol{k}_{\rm T}\boldsymbol{x}_{\rm T}}\, S_P(k \approx k_{\rm L}, \boldsymbol{k}_{\rm T}). \quad (47)$$

Eq. (47) gives us a good tool to investigate the space-time structure of DLA. We may now concentrate on particle distribution in transverse coordinates, which is physically the most interesting case. For the sake of simplicity, let us consider for $t = 0$ the single particle amplitude $S_P(k, \boldsymbol{x}_{\rm T})$ in mixed transverse space and longitudinal momentum coordinates [14] defined as:

$$S_P(k_{\rm L} \approx k, \boldsymbol{x}_{\rm T}, 0) = \int d^2k_{\rm T}\, e^{-i\boldsymbol{k}_{\rm T}\boldsymbol{x}_{\rm T}} S_P(k_{\rm L} \approx k, \boldsymbol{k}_{\rm T}). \quad (48)$$

For the single particle exclusive distribution $\rho_P^{\rm ex}(k, \boldsymbol{x}_{\rm T}, 0)$, defined as the amplitude square:

$$\rho_P^{\rm ex}(k, \boldsymbol{x}_{\rm T}, 0) \ = \mid S_P(k, \boldsymbol{x}_{\rm T}, 0) \mid^2 \quad (49)$$

one obtains simple expression in the form:

$$\begin{aligned} \rho_P^{\rm ex}(k, \boldsymbol{x}_{\rm T}, 0) &= \frac{1}{(2\pi)^2} \int d^2k_{\rm T} d^2k'_{\rm T}\, {\rm e}^{-i(\boldsymbol{k}_{\rm T}-\boldsymbol{k}'_{\rm T})\boldsymbol{x}_{\rm T}}\, S_P(k, {\rm k}_{\rm T}) S_P^*(k, {\rm k}'_{\rm T}) \\ &= \frac{1}{(2\pi)^2} \int d^2k_{\rm T} d^2k'_{\rm T}\, {\rm e}^{-i(\boldsymbol{k}_{\rm T}-\boldsymbol{k}'_{\rm T})\boldsymbol{x}_{\rm T}}\, d_P^{\rm ex}(k, \boldsymbol{k}'_{\rm T}; k, \boldsymbol{k}_{\rm T}). \quad (50) \end{aligned}$$

Relation (50) holds also for inclusive single particle density (for proof see Appendix G):

$$\rho_P^{\rm in}(k, \boldsymbol{x}_{\rm T}, 0) \ = \ \frac{1}{(2\pi)^2} \int d^2k_{\rm T} d^2k'_{\rm T}\ {\rm e}^{-i(\boldsymbol{k}_{\rm T}-\boldsymbol{k}'_{\rm T})\boldsymbol{x}_{\rm T}}\ d_P^{\rm in}(k, \boldsymbol{k'}_{\rm T}; k, \boldsymbol{k}_{\rm T}) \quad (51)$$

and can be easily generalized for any multiparticle distributions. In this paper we study the inclusive single particle density in mixed coordinates $\rho_P^{\rm in}(k, \boldsymbol{x}_{\rm T}, 0)$ for the QCD gluonic cascade in DLA approximation.

4. Inclusive single particle density in configuration space

4.1. Physics

Momentum and configuration space description of a particle source are related to each other by the Fourier transform. Therefore one expects to extract from the observables in momentum space some qualitative information about their behaviour in configuration space. This observation applies, of course, to single particle density. In the DLA approach the inclusive single particle density $\rho_P^{\rm in}(\boldsymbol{k})$ [12] reads:

$$\begin{aligned}\rho_P^{\rm in}(\boldsymbol{k}) &= \frac{2b}{2\pi}\frac{1}{kk_{\rm T}^2}\sum_{n=0}^{\infty}\frac{(2b)^n}{(n!)^2}\ln^n\Big(\frac{P}{k}\Big)\ln^n\Big(\frac{k_{\rm T}}{Q_0}\Big)\,\Theta_P(k)\\ &= \frac{2b}{2\pi}\frac{1}{kk_{\rm T}^2}I_0\left(\sqrt{8b\,\ln\Big(\frac{P}{k}\Big)\ln\Big(\frac{k_{\rm T}}{Q_0}\Big)}\right)\,\Theta_P(k);\end{aligned} \tag{52}$$

where $b \equiv g_S^2 C_{\rm F}$. For constant k the $\rho_P^{\rm in}(\boldsymbol{k})$ is concentrated around $\boldsymbol{P}$ direction (see Fig. 6)(skipping for now the $\Theta_P(k)$ limitations). We expect, that the single particle distribution $\rho_P^{\rm in}(t, \boldsymbol{x})$ in configuration space:

$$\rho_P^{\rm in}(k, \boldsymbol{x}_{\rm T}, 0) = \frac{1}{(2\pi)^2}\int d^2k_{\rm T}d^2k'_{\rm T}\,{\rm e}^{-i(\boldsymbol{k}_{\rm T}-\boldsymbol{k}'_{\rm T})\boldsymbol{x}_{\rm T}}\;d_P^{\rm in}(k, \boldsymbol{k}'_{\rm T}; k, \boldsymbol{k}_{\rm T}) \tag{53}$$

will be concentrated around the P direction, as well. However, it has to obey the uncertainty principle. Since there are cut-offs of form (9) in density matrix, its Fourier transform will contain some oscillations, due to the

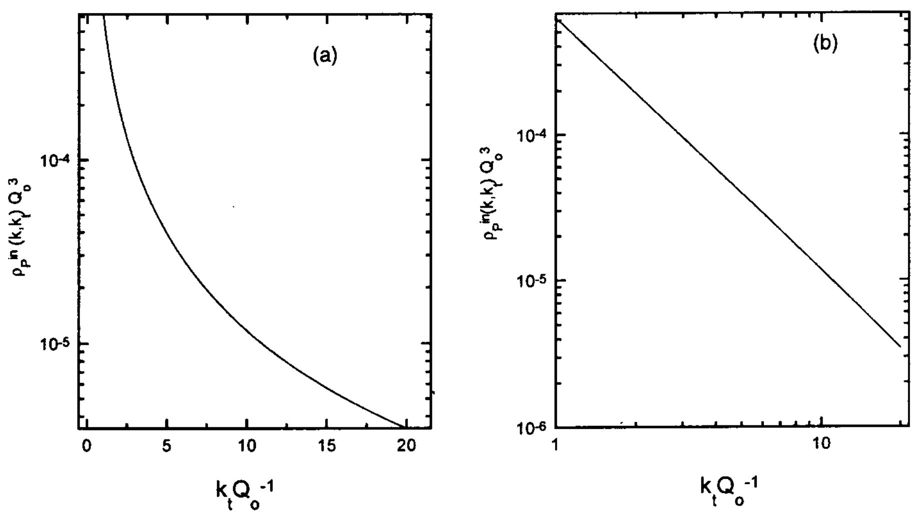

Fig. 6. Function $\rho_P^{\rm in}(\boldsymbol{k})$ from Eq. (52) *vs* $k_{\rm T} \equiv|\boldsymbol{k}_{\rm T}|$ in Q_0 units for parameters $b = 0.25$, $P/Q_0 = 243$, $\theta = 1$, $k/Q_0 = 128$, chosen following [12]. The power fit reads $\rho_P^{\rm in}(\boldsymbol{k}) = (k_{\rm T}/Q_0)^{-1.74} * 0.00065\,Q_0^{-3}$. Plot (a) with the logarithmic scale for the vertical axis, plot (b) with the logarithmic scale for both vertical and horizontal axes.

restricted integration region. Moreover, relation (6) implies, that both densities $\rho_P^{\rm in}(\boldsymbol{k})$ and $\rho_P^{\rm in}(k, \boldsymbol{x}_{\rm T}, 0)$ have the same normalization, if integrated over d^3k and $dk\, d^2x_{\rm T}$ respectively.

Remembering the above remarks, we propose now a technique for deriving the explicit form of inclusive single particle density in configuration space.

4.2. Single particle density

We may calculate the single particle density $\rho_P^{\rm in}(k, \boldsymbol{x}_{\rm T}, 0)$ as a Fourier transform of DLA density matrix (43). Let us make the transverse Fourier transform of both sides of Eq. (43). We obtain:

$$\begin{aligned}
&\rho_P^{\rm in}(k, \boldsymbol{x}_{{\rm T}(\boldsymbol{P})}, 0) \\
&= \frac{1}{(2\pi)^2}\int d^2k_{T(P)} d^2k_{T(P)}\, {\rm e}^{-i(\boldsymbol{k}_{{\rm T}(P)}-\boldsymbol{k}'_{{\rm T}(P)})\boldsymbol{x}_{T(P)}}\, d_P^{\rm in}(k, \boldsymbol{k}'_{\rm T}; k, \boldsymbol{k}_{\rm T}) \\
&\overset{\rm DLA}{=} \frac{1}{(2\pi)^2}\int d^2k_{T(P)} d^2k'_{T(P)} e^{-i(\boldsymbol{k}_{{\rm T}(P)}-\boldsymbol{k}'_{T(P)})\boldsymbol{x}_{{\rm T}(P)}} \\
&\times \sum_{n=0}^{\infty}(2b)^n \int\frac{ds_1}{s_1}\int\frac{d\Omega_{s_1}}{2\pi\theta_{P1}^2}\Theta_P(s_1)\ldots\int\frac{ds_n}{s_n}\int\frac{d\Omega_{s_n}}{2\pi\theta_{n-1,n}^2}\Theta_{s_{n-1}}(s_n) \\
&\times g_{s_n}^{(1)}(k, \boldsymbol{k}'_{{\rm T}(\boldsymbol{S})}; k, \boldsymbol{k}_{{\rm T}(\boldsymbol{S})}); \qquad (54)
\end{aligned}$$

where indices T(P),T(S) correspond to the reference frame with the z−axis placed along the P (S) direction. The term of the lowest order ($n = 0$) takes then the form:

$$\begin{aligned}
&\rho_P^{in\,(1)}(k, \boldsymbol{x}_{{\rm T}(P)}, 0) \\
&= \frac{1}{(2\pi)^2}\int d^2k_{T(P)} d^2k'_{T(P)}\, {\rm e}^{-i(\boldsymbol{k}_{{\rm T}(P)}-\boldsymbol{k}'_{T(P)})\boldsymbol{x}_{{\rm T}(P)}}\, g_P^{(1)}(k, \boldsymbol{k}_{{\rm T}(S)}; k, \boldsymbol{k}_{{\rm T}(S)}) \\
&= \frac{2b}{2\pi}k\,\Theta(\frac{Q_0}{\theta} < k < P)(\int_{\frac{Q_0}{k}}^{\theta} d\theta_{Pk} J_0(x_{\rm T} k\theta_{Pk}))^2. \qquad (55)
\end{aligned}$$

The numerical plot of (55) is presented in Fig. 7. There is a limiting maximum value for $x_{\rm T} = 0$, as expected, and for large $x_{\rm T}$ the function has a power decrease with the best fit exponent $x_{\rm T}^{-3.07}$. The result confirms our intuitive analysis from Section 4. 1. The term $\rho_P^{\rm in\,(1)}(k, \boldsymbol{x}_{{\rm T}(P)}, 0)$ is concentrated around the $\boldsymbol{P}$ direction, however stronger than $\rho_P^{\rm in\,(1)}(k, \boldsymbol{k}_{\rm T})$ from Eq. (52).

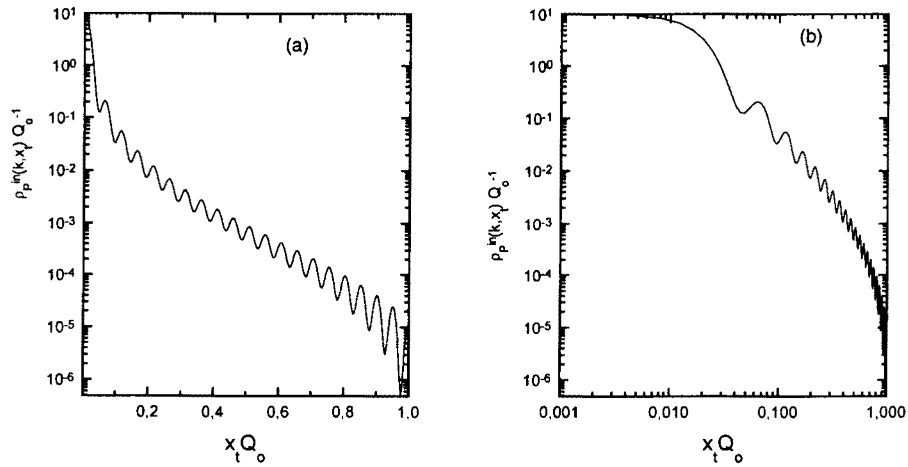

Fig. 7. Function $\rho_P^{\mathrm{in},(1)}(k,\boldsymbol{x}_\mathrm{T},0)$ from Eq. (55) *vs* $x_\mathrm{T} \equiv \mid \boldsymbol{x}_\mathrm{T} \mid$ for parameters as in Fig. 6. The power fit reads $\rho_P^{\mathrm{in}}(k,\mathbf{x}_\mathrm{T},0) = (Q_0 x_\mathrm{T})^{-3.07} * 4.0E-05\,Q_0$. Plot (a) with the logarithmic scale for the vertical axis, plot (b) with the logarithmic scale for both vertical and horizontal axes.

Derivation of terms of an arbitrary order in expansion (43) is more complicated. To proceed, let us analyse the last part of (43). It reads:

$$\begin{aligned}&\int \frac{ds_n}{s_n} \int \frac{d\Omega_n}{2\pi\theta^2_{n-1,n}}\,\Theta_{n-1}(s_n)\,g_n^{(1)}(k,\boldsymbol{k}'_{\mathrm{T}(S)};k,\boldsymbol{k}_{\mathrm{T}(S)})\\ &= \frac{2b}{2\pi k^3}\int \frac{ds_n}{s_n}\int \frac{d\Omega_n}{2\pi\theta^2_{n-1,n}}\,\Theta_{n-1}(s_n)\frac{1}{\theta_{nk'}\theta_{nk}}\,\Theta_n(k')\Theta_n(k), \qquad (56)\end{aligned}$$

where the index (i) refers to the vector $\boldsymbol{s}_i$. Taking into account phase space restriction and dominating contribution of $1/(\theta_{nk'}\theta_{nk})$ (see Appendix E) expression (56) can be approximated as:

$$\begin{aligned}&\frac{2b}{2\pi k^3}\int \frac{ds_n}{s_n}\int \frac{d\Omega_n}{2\pi\theta^2_{n-1,n}}\,\Theta_{n-1}(s_n)\frac{1}{\theta_{nk'}\theta_{nk}}\,\Theta_n(k')\Theta_n(k)\\ &= \frac{2b}{2\pi k^3}\ln(\frac{s_{n-1}}{k})\frac{1}{\theta_{n-1,k'}\theta_{n-1,k}}\Theta_{n-1}(k')\Theta_{n-1}(k)\\ &\times \int\limits_0^\infty dx_n x_n J_0(x_n\theta_{kk'}) \int\limits_{\frac{Q_0}{k}}^{\theta_{n-1,k}} d\theta_{nk} J_0(x_n\theta_{nk}) \int\limits_{\frac{Q_0}{k}}^{\theta_{n-1,k'}} d\theta_{nk'} J_0(x_n\theta_{nk'})\,. \qquad (57)\end{aligned}$$

Scheme (57) can be repeated iteratively in (43). After some transformations one obtains finally (for details see Appendix E, H):

$$
\begin{aligned}
&\rho_P^{\rm in}(k,\boldsymbol{x}_{\mathrm{T}(P)},0)\\
&= \frac{2b}{2\pi}\, k\,\Theta\left(\frac{Q_0}{\theta}<k<P\right)\int\limits_{\frac{Q_0}{k}}^{\theta} d\theta_{Pk}\int\limits_{\frac{Q_0}{k}}^{\theta} d\theta_{Pk'}\,\frac{1}{2\pi}\int\limits_{0}^{2\pi} d\varphi_{k'k}\, J_0(k\theta_{k'k}x_{\mathrm{T}})\\
&\times I_0\left(\sqrt{8b\,\ln\left(\frac{P}{k}\right)\left\{\int_0^{\infty} dx\,x J_0(x\theta_{kk'})\int_{\frac{Q_0}{k}}^{\theta_{Pk}} da J_0(xa)\int_{\frac{Q_0}{k}}^{\theta_{Pk'}} da' J_0(xa')\right\}}\right)\\
&= \frac{2b}{2\pi}\, k\,\Theta\left(\frac{Q_0}{\theta}<k<P\right)\\
&\times \int\limits_{\frac{Q_0}{k}}^{\theta} d\theta_{Pk}\int\limits_{\frac{Q_0}{k}}^{\theta} d\theta_{Pk'}\,\frac{1}{2\pi}\int\limits_{0}^{\infty}\frac{d\theta_{k'k}\,\theta_{k'k}}{\Delta(\theta_{Pk},\theta_{Pk'},\theta_{k'k})}J_0(k\theta_{k'k}x_{\mathrm{T}})\\
&\times I_0\left(\sqrt{8b\,\ln\left(\frac{P}{k}\right)\left\{\int_{\frac{Q_0}{k}}^{\theta_{Pk}} da\int_{\frac{Q_0}{k}}^{\theta_{Pk'}} da'\frac{1}{2\pi\Delta(a,a',\theta_{k'k})}\right\}}\right)\,, \qquad (58)
\end{aligned}
$$

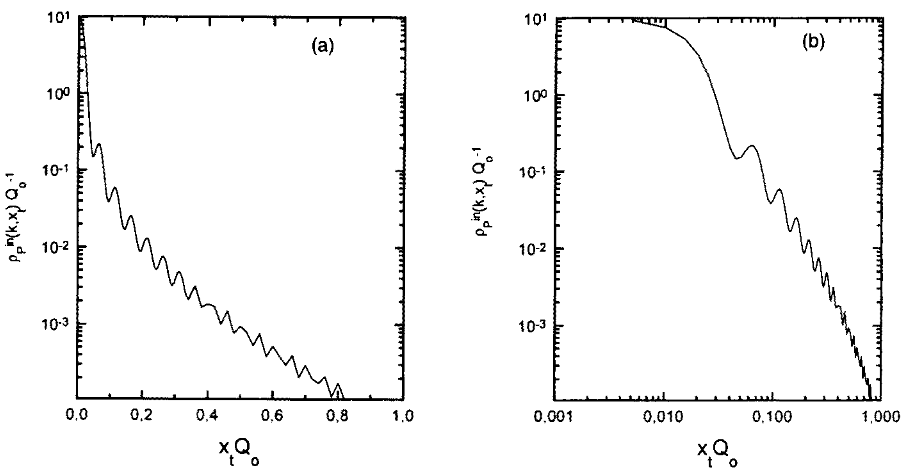

Fig. 8. Function $\rho_P^{\rm in}(k,\boldsymbol{x}_{\mathrm{T}},0)$ from Eq. (58) *vs* $x_{\mathrm{T}}\equiv\mid\boldsymbol{x}_{\mathrm{T}}\mid$ for parameters as in Fig. 6. Plot (a) with the logarithmic scale for the vertical axis, plot (b) with the logarithmic scale for both vertical and horizontal axes. The power fit reads $\rho_P^{\rm in}(k,\boldsymbol{x}_{\mathrm{T}},0)=(Q_0x_{\mathrm{T}})^{-2.43}*0.00018\,Q_0$.

where $\theta_{k'k}$ denotes the angle between momenta $\boldsymbol{k}'$, $\boldsymbol{k}$, which in the reference frame with the z-axis placed along P direction takes the simple form:

$$\theta_{k'k} = \sqrt{\theta_{Pk'}^2 + \theta_{Pk}^2 - 2\,\theta_{Pk'}\theta_{Pk}\cos(\varphi_{k'k})} \tag{59}$$

$\varphi_{k'k}$ denotes the azimuthal angle between $\boldsymbol{k}_{\mathrm{T}}$ and $\boldsymbol{k}'_{\mathrm{T}}$, and $\Delta(a,b,c)$ denotes the area of the triangle with sides a, b, c. The numerical plot of (58) is presented in Fig. 8. There is a limiting maximum value for $x_{\mathrm{T}} = 0$, as expected, and for large x_{T} the function has a power decrease with the best fit exponent $x_{\mathrm{T}}^{-2.43}$. The result confirms our intuitive analysis from Sec. 4. 1. The term $\rho_P^{\mathrm{in}\,(1)}(k, \boldsymbol{x}_{\mathrm{T}(P)}, 0)$ is concentrated around the $\boldsymbol{P}$ direction, stronger than $\rho_P^{\mathrm{in}\,(1)}(k, \boldsymbol{k}_{\mathrm{T}})$ from Eq. (52). The function oscillates around its power-law profile. As already mentioned in Section 4. 1., this effect is due to the sharp cut-offs of form (9) which restrict the integration space.

4.3. Properties

Let us analyse the properties of (58) in detail. Comparing (58) with the single particle density in momentum space (52), we get the same dependence on the energy k, as expected. The complicated emission term (see Fig. 9):

$$2b\,\ln\left(\frac{P}{k}\right)\left\{\int_0^\infty dx\,x J_0(x\theta_{kk'})\int_{\frac{Q_0}{k}}^{\theta_{Pk}} da J_0(xa)\int_{\frac{Q_0}{k}}^{\theta_{Pk'}} da' J_0(xa')\right\}$$
$$= \int d^3s\,\frac{k^3}{s^3}\,A_{ss}(k, \boldsymbol{k}'_{\mathrm{T}}; k, \boldsymbol{k}_{\mathrm{T}}) \tag{60}$$

corresponds to the logarithm $\ln k_{\mathrm{T}}/Q_0$ of (52). In fact, after integration of $\rho_P^{\mathrm{in}}(k, \boldsymbol{x}_{\mathrm{T}(P)}, 0)$ over d^2x_{T} one obtains the same result as for (52) integrated

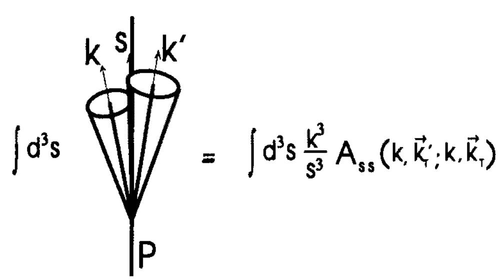

Fig. 9. Diagramatic representation of the term (60). The integration region lies in the overlap of conus $\Theta_s(k)$ and conus $\Theta_s(k')$.

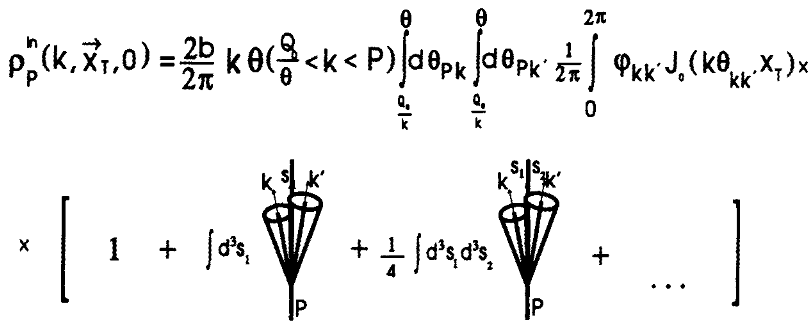

Fig. 10. Diagramatic representation of $\rho_P^{\rm in}(k, \boldsymbol{x}_{\rm T}, 0)$ from Eq. (58) as the chain of independent emission factors (60) transformed onto the transverse $x_{\rm T}$ plane by the Bessel factor of primary emission from the parent P, namely $J_0(\mid \boldsymbol{k}_{\rm T} - \boldsymbol{k}'_{\rm T} \mid x_{\rm T})$.

over $d^2k_{\rm T}$ (see Appendix I). The density $\rho_P^{\rm in}(k, \boldsymbol{x}_{\rm T}(P), 0)$ is positively defined, as well. Using the Bessel function identities from Appendix H, Eq. (58) can be rewritten in the form:

$$\begin{aligned}
&\rho_P^{\rm in}(k, \boldsymbol{x}_{\rm T}(P), 0) \\
&= \frac{2b}{2\pi} k\Theta(\frac{Q_0}{\theta} < k < P) \sum_{n=0}^{\infty} \frac{(2b)^n}{(n!)^2} \ln^n \frac{P}{k} \left(\int_0^\infty dx_1 x_1 ... \int_0^\infty dx_n x_n \right) \\
&\times \sum_{m_1..m_n=-\infty}^{\infty} \left\{ \int_{\frac{Q_0}{k}}^{\theta} d\theta_{Pk} J_{m_1}(x_1\theta_{Pk})...J_{m_n}(x_n\theta_{Pk})\, J_{m_1+...+m_n}(x_{\rm T} k\theta_{Pk}) \right. \\
&\left. \times \prod_{i=1}^{n} \int_{\frac{Q_0}{k}}^{\theta_{Pk}} da_i J_0(x_i a_i) \right\}^2 \qquad (61)
\end{aligned}$$

which implies positive definitness. For $x_{\rm T} = 0$ $\rho_P^{\rm in}(k, \boldsymbol{x}_{{\rm T}(P)}, 0)$ reaches its maximal value, as expected. Diagramatically, formula (58) represents the chain of independent emission factors (60) transformed onto the transverse $x_{\rm T}$ plane by the Bessel factor of primary emission from the parent P, namely $J_0(\mid \boldsymbol{k}_{\rm T} - \boldsymbol{k'}_{\rm T} \mid x_{\rm T})$ (see Fig. 10). For $k = P$ expression (58) reduces to (55) with the dominance of the primary emission, as expected.

5. Summary

We considered the QCD parton cascade created in e^+e^- collision in the double logarithmic approximation. Using the density matrix (DM) formalism [10], and restricting ourselves to the terms leading in the double logarithmic (DL) perturbative expansion for the quasi-diagonal limit $k' \cong k$, we derived the explicit form of the inclusive single particle density matrix $d_P^{\rm in}(k', k)$ and single particle density $\rho_P^{\rm in}(k, \boldsymbol{x}_{{\rm T}(P)}, 0)$ (see Fig. 8) in mixed coordinates $(k_{\rm L} \approx k, \boldsymbol{x}_{\rm T})$. The gluon density $\rho_P^{\rm in}(k, \boldsymbol{x}_{{\rm T}(P)}, 0)$ fulfills important physical requirements such as positive definitness and proper normalization. It is concentrated around the $\boldsymbol{P}$ direction, and shows the power law profile for large $\boldsymbol{x}_{\rm T}$. Due to the cut-offs of the type (9) which restrict kinematic regions, the density oscillates around its power law profile.

The above results give a positive outlook for the future. The simplified technique for calculating multiparticle observables in DLA for the constant α_S is ready. It may allow one to investigate the structure of the QCD cascade in a very comprehensive way: the exact form of a Wigner function already would give us clear experimental predictions.

In order to improve the approach one needs to include the momentum dependence of α_S. The exact analysis of applicability of the quasi-diagonal approximation $k' \cong k$ would be required, as well. There is also a problem as to what extent the kinematical constraints characteristic for a given QCD approach (in DLA they are of the form (9)) influence the results obtained in the approach. In other words, there is a problem how to separate the effects of the kinematical restriction from the dynamical content of QCD space. The explanation would require performing an analysis similar to the presented above for LLA and MLLA schemes, as well. The MLLA approximation would be of special interest since it would incorporate the energy conservation into the cascade.

I would like to express my deep gratitude to Professor Andrzej Bialas for the encouragement to study the subject of this work, for many helpful discussions and suggestions, and a continuous interest and support throughout this work. I would like to thank Professor Jacek Wosiek for many supportive and enlightening discussions and comments, for careful reading the manuscripts, and for his continued interest of this work. I am greatly indebted to Professor Alberto Giovannini for interesting comments and suggestions concerning this work and the positive outlook for the future. I would like to thank the organizers of the XXXVII Cracow School of Theoretical Physics for their invitation and warm hospitality.

Appendix A

The functionals $Z_P[u]$ and $Z_{P'}[s]$ defined in (19) generate the sum of amplitudes (7) and their complex conjugates over all possible tree diagrams respectively. It can be seen when one rewrites the master equation for Z_P in the form of the diagram series (see Fig. 2). From that construction follows exclusive density matrix (20):

$$d_P^{\rm ex}(\boldsymbol{k}'_1,..,\boldsymbol{k}'_m;\boldsymbol{k}_1,..,\boldsymbol{k}_m) = \frac{\delta^m}{\delta s_{1'}...\delta s_{m'}} Z_P^*[s]\,|_{\{s=0\}}\, \frac{\delta^m}{\delta u_1...\delta u_m} Z_P[u]\,|_{\{u=0\}}\,. \tag{62}$$

Then the inclusive density matrix calculated from (3) looks like this:

$$d_P^{\rm in}(\boldsymbol{k}'_1,..,\boldsymbol{k}'_m;\boldsymbol{k}_1,..,\boldsymbol{k}_m) = \sum_{n=0}^{\infty} \frac{1}{n!}\left(\int d^3k \frac{\delta}{\delta s}\frac{\delta}{\delta u}\right)^n \frac{\delta^m}{\delta s_{1'}...\delta s_{m'}} Z_P^*[s]\,|_{\{s=0\}} \times \frac{\delta^m}{\delta u_1...\delta u_m} Z_P[u]\,|_{\{u=0\}} \tag{63}$$

and from the identity for the product of any two functionals F, F':

$$F[u]F'[w]\,|_{\{u=\frac{\delta}{\delta w},w=0\}} = \sum_{n=0}^{\infty} \frac{1}{n!}\left(\int d^3k \frac{\delta}{\delta w}\frac{\delta}{\delta u}\right)^n F[u]\,|_{\{u=0\}}\, F'[w]\,|_{\{w=0\}} \tag{64}$$

follows (21).

Appendix B

In DLA there are four different tree graphs M_a, M_b, M_c, M_d, describing the production of two gluons. They are defined on non-overlapping kinematic regions (see Fig. 3). Emitted gluons are either angular (AO) or energy ordered (EO).

Let us consider all the diagrams contributing to the single particle density matrix $d_P^{\rm ex}(k'_1, k_1)$. From the (AO) and (EO) it follows that the interference between any two different graphs will appear only if either energies ω_1, ω'_1 or emission angles $\theta_{1P}, \theta_{1'P}$ of produced gluons are *strongly* ordered (Fig. 4).

This statement can be generalized for any m-particle density matrix by induction. If we have m particles, and (m-1) ones among them are "close" to each other, *i.e.* $k_1 \cong k'_1, ..., k_{m-1} \cong k'_{m-1}$, then the interference of the different diagrams will take place only if either energies or angles of k_m and k'_m are strongly ordered.

Appendix C

$Z_{P'P}[u(k',k)]$ defined in (26) generates correct exclusive density matrices (24). The proof of this statement follows from the representation of the master equation for $Z_{P'P}$ as a diagram series (see Fig. 5). The series reproduces all squared contributions of identical tree diagrams, and excludes interference of the different ones (function $P_{1',\ldots,n';1,\ldots,n}$).

The explicit form of inclusive density (25) follows from formula (3). Substituting (24) into (3) one obtains:

$$d_P^{\rm in}(\boldsymbol{k}'_1,..,\boldsymbol{k}'_m;\boldsymbol{k}_1,..,\boldsymbol{k}_m)$$
$$= \sum_{n=0}^{\infty}\frac{1}{n!}\left(\int d^3k d^3k' \delta^3(k'-k)\frac{\delta}{\delta u_{k',k}}\right)^n \frac{\delta^m}{\delta u_{m',m}...\delta u_{1',1}} Z_{P'P}[u]\mid_{\{u=0\}}; \tag{65}$$

which represents the functional $Z_{P'P}[u]$ expanded around "null" $\{u=0\}$ in the "point" $u=\delta^3(l'-l)$.

Appendix D

We want to average relation (28) over physical polarizations. The exact expression to be summed over polarizations looks like this:

$$\frac{(e\cdot P)(e'\cdot P')}{(k\cdot P)(k'\cdot P')}, \tag{66}$$

where e, e' are polarizations of the same gluon identical in the limit $k'=k$. The gauge fixing we apply in the approach allows us to neglect contributions to (66) coming from the "nonphysical" polarizations e^0 and e^3. Furthermore, it requests the time components of the physical polarizations e^1, e^2 to be equal to 0. Space components of e^1, e^2 can be then constructed in the form:

$$\begin{aligned} \boldsymbol{e}^2 &= \frac{\boldsymbol{P}\times\boldsymbol{k}}{\mid\boldsymbol{P}\times\boldsymbol{k}\mid}, \\ \boldsymbol{e}^1 &= \frac{\boldsymbol{e}^2\times\boldsymbol{k}}{\mid\boldsymbol{e}^2\times\boldsymbol{k}\mid}; \end{aligned} \tag{67}$$

and for e' respectively:

$$\begin{aligned} \boldsymbol{e}'^2 &= \frac{\boldsymbol{P}'\times\boldsymbol{k}'}{\mid\boldsymbol{P}'\times\boldsymbol{k}'\mid}, \\ \boldsymbol{e}'^1 &= \frac{\boldsymbol{e}'^2\times\boldsymbol{k}'}{\mid\boldsymbol{e}'^2\times\boldsymbol{k}'\mid}. \end{aligned} \tag{68}$$

Summing over these 2 polarizations and expanding scalar products in (66), one obtains finally:

$$\sum_{j=1,2} \frac{(e^j \cdot P)(e'^j \cdot P')}{(k \cdot P)(k' \cdot P')} = \frac{4}{\omega\omega'} \frac{1}{\theta_{Pk}\theta_{P'k'}}. \tag{69}$$

The result can be easily confirmed for any two physical polarizations $\varepsilon^1, \varepsilon^2$ placed on the plane $\boldsymbol{e}^1\boldsymbol{e}^2$:

$$\begin{aligned} \varepsilon^1 &= \cos\varphi\, \boldsymbol{e}^1 + \sin\varphi\, \boldsymbol{e}^2 , \\ \varepsilon^2 &= -\sin\varphi\, \boldsymbol{e}^1 + \cos\varphi\, \boldsymbol{e}^2; \end{aligned} \tag{70}$$

and for $\boldsymbol{\varepsilon}'^1, \boldsymbol{\varepsilon}'^2$ placed on the plane $\boldsymbol{e}'^1\boldsymbol{e}'^2$ with the phases $\varphi' = \varphi$ respectively.

Appendix E

To transform (56) into (57) we will apply the pole approximation method (see [12] and references therein). The phase space restrictions $\Theta_{n-1}(n)\,\Theta_n(k)\,\Theta_{n'}(k')$ in (56), in particular the angular ordering (AO) $\theta_{n-1,n} \gg \theta_{n,k}, \theta_{n-1,n} \gg \theta_{n,k'}$ make the the term $1/\theta_{nk'}\theta_{nk}$ be dominating in (56). Applying the Bessel function identity [14]:

$$\begin{aligned} \int \frac{d\Omega_n}{2\pi} &= \frac{1}{2\pi} \int \frac{d\theta_{nk}\, d\theta_{nk'}\, \theta_{nk}\, \theta_{nk'}}{\Delta(\theta_{nk}, \theta_{nk'}, \theta_{kk'})} \\ &= \int_0^\infty dx x J_0(x\theta_{k'k}) \int d\theta_{nk}\theta_{nk}\, J_0(x\theta_{nk}) \int d\theta_{nk'}\theta_{nk'}\, J_0(x\theta_{nk'}), \end{aligned} \tag{71}$$

where $\theta_{k'k}$ denotes the relative angle between $\boldsymbol{k}, \boldsymbol{k}'$, and $\Delta(\theta_{nk}, \theta_{nk'}, \theta_{kk'})$ equals the area of triangle with sides $\theta_{k'k}$, $\theta_{k'n}$, θ_{kn}, we may rewrite expression (56) in the form:

$$\begin{aligned} &\frac{2b}{2\pi k^3} \int \frac{ds_n}{s_n} \int \frac{d\Omega_n}{2\pi\theta^2_{n-1,n}} \Theta_{n-1}(n) \frac{1}{\theta_{nk'}\theta_{nk}} \Theta_n(k')\Theta_n(k) \\ &= \frac{2b}{2\pi k^3} \int \frac{ds_n}{s_n} \int_0^\infty dx_n x_n J_0(x_n\theta_{kk'}) \int d\theta_{nk} J_0(x_n\theta_{nk}) \int d\theta_{nk'} J_0(x_n\theta_{nk'}) \\ &\times \frac{1}{\theta^2_{n-1,n}} \Theta_{n-1}(n)\Theta_n(k')\Theta_n(k). \end{aligned} \tag{72}$$

Because of angular ordering the angle $\theta_{n-1,n}$ practically does not change while integrating over angles $\theta_{nk}, \theta_{nk'}$, and can be successfully approximated by the angle $\theta_{n-1,k}$ $(\theta_{n-1,k'})$. Applying all the integration restrictions explicitly, we arrive finally at the expression:

$$\frac{2b}{2\pi k^3}\int\frac{ds_n}{s_n}\int\frac{d\Omega_n}{2\pi\theta^2_{n-1,n}}\Theta_{n-1}(n)\frac{1}{\theta_{nk'}\theta_{nk}}\Theta_n(k')\Theta_n(k)$$
$$=\frac{2b}{2\pi k^3}\frac{1}{\theta_{n-1,k'}\theta_{n-1,k}}\Theta_{n-1}(k')\Theta_{n-1}(k)\int\limits_{k}^{s_{n-1}}\frac{ds_n}{s_n}$$
$$\times\int\limits_0^\infty dx_n x_n J_0(x_n\theta_{kk'})\int\limits_{\frac{Q_0}{k}}^{\theta_{n-1,k}}d\theta_{nk}J_0(x_n\theta_{nk})\int\limits_{\frac{Q_0}{k}}^{\theta_{n-1,k'}}d\theta_{nk'}J_0(x_n\theta_{nk'}) \quad (73)$$

which after trivial integration over s_n gives identity (57).

Appendix F

We shall find such terms in expansion (36) which dominate in the double logarithmic perturbative limit of $d_P^{\rm in}(k',k)$, *i.e.* when $b\to 0$ ($b\propto\alpha_S$) and $P\to\infty$, so that $b\ln^2\frac{P}{Q_0}$ remains constant, and generate double logarithmic corrections to the cross-section. First let us introduce the following notation:

$$d_P^{\rm in}(k',k)=\sum_{n=0}^{\infty}a_n; \quad (74)$$

where coefficients a_n describe the n-th order iteration of $g_S(k',k)$ (36) in the form:

$$a_n=(2b)^n\int\frac{ds_1}{s_1}\int\frac{d\Omega_{s_1}}{2\pi\theta^2_{Ps1}}\Theta_P(s_1)...$$
$$\times\int\frac{ds_n}{s_n}\int\frac{d\Omega_{s_n}}{2\pi\theta^2_{n-1,n}}\Theta_{s_{n-1}}(s_n)\,g_{s_n}(k',k). \quad (75)$$

The term a_0 of the series (75) is equal to $g_P(k',k)$. Expanding it in the powers of coupling constant b, one obtains the term of the first (lowest) order of b in the form:

$$a_0^{(1)}\equiv g_P^{(1)}(k',k)=\frac{2b}{2\pi}\frac{1}{\sqrt{k^3k'^3}}\frac{1}{\theta_{Pk'}\theta_{Pk}}\Theta_P(k')\,\Theta_P(k). \quad (76)$$

Denoting the other terms by the symbol $a_0^{(>1)}\equiv g_P^{(>1)}(k',k)$, the term a_0 from the series (75) can be rewritten as:

$$a_0=a_0^{(1)}+a_0^{(>1)}. \quad (77)$$

We have checked that $a_0^{(1)}$ dominates in (77). To see this, one should rewrite a_0 as:

$$a_0 \equiv g_P(k',k) = a_0^{(1)} + a_0^{(>1)} \tag{78}$$

$$= a_0^{(1)} f(k',k;P), \tag{79}$$

where the exact form of $f(k',k;P)$ follows from (37). For $b > 0$ and P finite the $f(k',k;P)$ *vs* $\mid \boldsymbol{k} - \boldsymbol{k}' \mid$ is a gauss-like function with the maximum equal to 1 for $\boldsymbol{k} = \boldsymbol{k}'$ and a non-zero minimal value. In the DL perturbative limit: $f(k',k;P) \stackrel{\mathrm{PT}}{\rightarrow} 1$. Consequently, for any k, k', P:

$$a_0 \leq a_0^{(1)}, \tag{80}$$

$$\frac{a_0}{a_0^{(1)}} \stackrel{\mathrm{PT}}{\rightarrow} 1. \tag{81}$$

Since $a_0^{(1)}$ dominates in a_0, we expect that the iterations of $a_0^{(1)}$ will generate the leading contributions to the $d_P^{\mathrm{in}}(k',k)$. Let us introduce the notation:

$$d_P^{\mathrm{in},(1)}(k',k) = \sum_{n=0}^{\infty} a_n^{(1)}, \tag{82}$$

$$d_P^{\mathrm{in},(>1)}(k',k) = \sum_{n=0}^{\infty} a_n^{(>1)}, \tag{83}$$

where $a_n^{(>1)}$ and $a_n^{(1)}$ represent the result of n-th iteration (75) of $a_0^{(>1)}$ and $a_0^{(1)}$ respectively. From (80) immediately follows the relation:

$$a_n = a_n^{(1)} + a_n^{(>1)} \leq a_n^{(1)}. \tag{84}$$

Since $a_n \geq 0$, for the density matrix one obtains:

$$0 \leq d_P^{\mathrm{in}}(k',k) = d_P^{\mathrm{in},(1)}(k',k) + d_P^{\mathrm{in},(>1)}(k',k) \leq d_P^{\mathrm{in},(1)}(k',k). \tag{85}$$

In the limit $\mid \boldsymbol{k} - \boldsymbol{k}' \mid \rightarrow 0$ the density matrix $d_P^{\mathrm{in}}(k',k) \rightarrow d_P^{in,(1)}(k',k)$, and therefore:

$$\frac{d_P^{\mathrm{in}}(k',k)}{d_P^{\mathrm{in},(1)}(k',k)} \stackrel{\mathrm{PT}}{\rightarrow} 1. \tag{86}$$

For other (larger) values of $\mid \boldsymbol{k} - \boldsymbol{k}' \mid$ the contribution of $d_P^{\mathrm{in},(1)}(k',k)$ generally need not to dominate. However, taking into account the fact that the density matrix approach works only for the quasi-diagonal limit, we may identify the quasi-diagonal region with the region of the dominance of $d_P^{\mathrm{in},(1)}(k',k)$. Furthermore, since $d_P^{\mathrm{in},(>1)}(k,k) = 0$, the $d_P^{\mathrm{in},(1)}(k',k)$ generates all DL corrections to the cross-section. Hence we finally arrive at the relation (43).

Appendix G

The particle density $\rho_P^{\rm in}(k,\boldsymbol{x}_{\rm T},0)$ can be represented as:

$$\rho_P^{\rm in}(k,{\rm x}_{\rm T},0)=\sum_{n=1}^{\infty}\frac{1}{(n-1)!}\int dk_2 d^2x_{2T}...dk_n d^2x_{nT}\,\rho_P^{\rm ex}(k,\boldsymbol{x}_{\rm T},k_2,\boldsymbol{x}_{2T},k_n,\boldsymbol{x}_{nT}). \tag{87}$$

Representing the exclusive particle density as the square of multiparticle amplitudes, expressing the configuration space amplitudes as Fourier transforms of amplitudes in momentum space, and performing integration over $d^2x_{2T}...d^2x_{nT}$ finally one arrives at Eq. (51).

Appendix H

For our purposes let us quote the following identities for Bessel functions ([15] and references therein):

$$J_0(x\theta_{k'k}) = \sum_{m=-\infty}^{\infty} e^{im(\varphi-\varphi')}J_m(x\theta_{kP})J_m(x\theta_{k'P}), \tag{88}$$

$$e^{i\,k\,x\,\cos\varphi} = \sum_{m=-\infty}^{\infty} i^m e^{im\varphi}J_m(k\,x), \tag{89}$$

$$\int_0^{\infty} dx\, xJ_0(x\,a)J_0(x\,a') = \frac{\delta(a-a')}{a}, \tag{90}$$

where $\theta_{k'k}$ denotes the relative angle between momenta $\boldsymbol{k}'$ $\boldsymbol{k}$, which in the reference frame with the z-axis placed along P direction takes form (59), and $\varphi_{k'k}=\varphi-\varphi'$, where the angles φ, φ' denote the azimuthal angles of vectors $\boldsymbol{k}_{\rm T}$ and $\boldsymbol{k}'_{\rm T}$ on the transversal plane respectively.

Now let us repeat the scheme Eq.(56)→ Eq.(57) iteratively in (43). Then, after introducing the explicit form of Fourier transform we arrive at the expression:

$$\begin{aligned}
&\rho_P^{\rm in}(k,\boldsymbol{x}_{\rm T(P)},0)\\
&=\frac{1}{(2\pi)^2}\int d(k\theta_{kP})\,k\theta_{kP}\int d(k\theta_{kP})\,k\theta_{kP}\int_0^{2\pi}d\varphi\int_0^{2\pi}d\varphi'\\
&\times\exp\left(-ik\theta_{kP}x_{\rm T}\cos\varphi+ik\theta_{k'P}x_{\rm T}\cos\varphi'\right)\\
&\times\sum_{n=0}^{\infty}\frac{(2b)^n}{n!}\ln^n\left(\frac{P}{k}\right)\frac{2b}{2\pi k^3}\frac{1}{\theta_{Pk}\theta_{Pk'}}\Theta_P(k)\Theta_P(k')
\end{aligned}$$

$$\times \left(\int_0^\infty dx_1 x_1 J_0(x_1\theta_{k'k}) ... \int_0^\infty dx_n x_n J_0(x_n\theta_{k'k}) \right)$$

$$\times \left\{ \int_{\frac{Q_0}{k}}^{\theta_{Pk}} da_1 J_0(x_1 a_1) \int_{\frac{Q_0}{k}}^{\theta_{Pk'}} da_1' J_0(x_1 a_{1'}) ... \int_{\frac{Q_0}{k}}^{\theta_{n-1,k}} da_n J_0(x_n a_n) \int_{\frac{Q_0}{k}}^{\theta_{n-1,k'}} da_n' J_0(x_n a_n') \right\} . \quad (91)$$

It looks still quite complicated, however one can notice that the term in brackets:

$$\left\{ \int_{\frac{Q_0}{k}}^{\theta_{Pk}} da_1 J_0(x_1 a_1) \int_{\frac{Q_0}{k}}^{\theta_{Pk'}} da_1' J_0(x_1 a_{1'}) ... \int_{\frac{Q_0}{k}}^{\theta_{n-1,k}} da_n J_0(x_n a_n) \int_{\frac{Q_0}{k}}^{\theta_{n-1,k'}} da_n' J_0(x_n a_n') \right\} \quad (92)$$

which contains integration of $2n$ Bessel functions, simplifies significantly if one adds to (91) some extra off-diagonal terms, which are equal to 0 in the quasi-diagonal limit. Namely:

$$\{\,\} \overset{\text{DLA}}{=} \frac{1}{n!} \int_{\frac{Q_0}{k}}^{\theta_{Pk}} da_1 J_0(x_1 a_1) \int_{\frac{Q_0}{k}}^{\theta_{Pk'}} da_1' J_0(x_1 a_{1'}) ... \int_{\frac{Q_0}{k}}^{\theta_{Pk}} da_n J_0(x_n a_n) \int_{\frac{Q_0}{k}}^{\theta_{Pk'}} da_n' J_0(x_n a_n') . \quad (93)$$

Then expression (91) takes the simpler form:

$$\rho_P^{\text{in}}(k, \boldsymbol{x}_{\text{T}(P)}, 0) = \frac{2b}{2\pi} k \Theta(\frac{Q_0}{\theta} < k < P) \frac{1}{(2\pi)^2}$$

$$\times \int_{\frac{Q_0}{k}}^{\theta} d\theta_{kP} \int_{\frac{Q_0}{k}}^{\theta} d\theta_{k'P} \int_0^{2\pi} d\varphi \int_0^{2\pi} d\varphi' \exp\left(-ik\theta_{kP} x_{\text{T}} \cos\varphi + ik\theta_{k'P} x_{\text{T}} \cos\varphi'\right)$$

$$\times \sum_{n=0}^{\infty} \frac{(2b)^n}{(n!)^2} \ln^n\left(\frac{P}{k}\right) \left\{ \int_0^\infty dx x J_0(x\theta_{k'k}) \int_{\frac{Q_0}{k}}^{\theta_{Pk}} da J_0(xa) \int_{\frac{Q_0}{k}}^{\theta_{Pk'}} da' J_0(xa') \right\}^n . \quad (94)$$

Let us perform the integration over the angles φ, φ'. Replacing all the terms of the type $J_0(x\theta_{k'k})$ by their expansions (88), expanding then Fourier transforms in terms of (89), and performing the integration over φ, φ' explicitly, we arrive at (61).

However, the part of expression (61) containing Bessel functions can be rewritten as:

$$\left(\prod_{i=1}^{n}\sum_{m_i=-\infty}^{\infty} J_{m_i}(x_i\theta_{Pk})J_{m_i}(x_i\theta_{Pk'})\right) J_{m_1+..+m_n}(x_{\rm T}k\theta_{Pk})J_{m_1+..+m_n}(x_{\rm T}k\theta_{Pk'})$$

$$= \frac{1}{2\pi}\int_0^{2\pi} d\varphi_{k'k}\left(\prod_{i=1}^{n} J_0(x_i\theta_{k'k})\right) J_0(x_{\rm T}k\theta_{k'k}), \tag{95}$$

where $\varphi_{k'k}$ denotes the relative angle between the vectors $\boldsymbol{k}_{\rm T}, \boldsymbol{k}'_{\rm T}$ and $\theta_{k'k} = \sqrt{\theta^2_{Pk'} + \theta^2_{Pk} - 2\,\theta_{Pk'}\theta_{Pk}\cos(\varphi_{k'k})}$, as usual. Substituting (95) into (61) finally we obtain (58).

Appendix I

Let us investigate normalization of single particle density (58) in real space, *i.e.* the integral $\int d^2x_{\rm T}\rho_P^{\rm in}(k,\boldsymbol{x}_{\rm T},0)$. It reads:

$$\int d^2x_{\rm T}\rho_P^{\rm in}(k,\boldsymbol{x}_{\rm T},0)$$

$$= 2bk\Theta(\frac{Q_0}{\theta} < k < P)\left(\int_{\frac{Q_0}{k}}^{\theta} d\theta_{Pk}\int_{\frac{Q_0}{k}}^{\theta} d\theta_{Pk'}\frac{1}{2\pi}\int_0^{2\pi} d\varphi_{k'k}\right)\int_0^{\infty} dx_{\rm T}x_{\rm T}J_0(k\theta_{k'k}x_{\rm T})$$

$$\times I_0\left(\sqrt{8b\,\ln\left(\frac{P}{k}\right)\left\{\int_0^{\infty} dx x J_0(x\theta_{kk'})\int_{\frac{Q_0}{k}}^{\theta_{Pk}} da J_0(xa)\int_{\frac{Q_0}{k}}^{\theta_{Pk'}} da' J_0(xa')\right\}}\right). \tag{96}$$

The term $J_0(k\theta_{k'k}x_{\rm T})$ is the only part of expression (96) depending on $x_{\rm T}$. Integral $\int_0^{\infty} dx_{\rm T}x_{\rm T}J_0(k\theta_{k'k}x_{\rm T})$ can be performed, using identities (88),(90). It equals:

$$\int_0^{\infty} dx_{\rm T}x_{\rm T}J_0(k\theta_{k'k}x_{\rm T}) = 2\pi\,\delta(\varphi_{k'k})\frac{\delta(\theta_{kP}-\theta_{k'P})}{k^2\theta_{kP}}. \tag{97}$$

Substituting (97) into (96), and integrating over $\theta_{k'P}$ and $\varphi_{k'k}$, one arrives at:

$$\int d^2x_{\rm T}\rho_P^{\rm in}(k,\boldsymbol{x}_{\rm T},0) = \frac{2b}{k}\Theta\left(\frac{Q_0}{\theta} < k < P\right)\int_{\frac{Q_0}{k}}^{\theta}\frac{d\theta_{Pk}}{\theta_{Pk}}$$

$$\times I_0\left(\sqrt{8b\,\ln\left(\frac{P}{k}\right)\left\{\int_0^\infty dx x\int_{\frac{Q_0}{k}}^{\theta_{Pk}} da J_0(xa)\int_{\frac{Q_0}{k}}^{\theta_{Pk}} da' J_0(xa')\right\}}\right). \tag{98}$$

Performing the integration over x in the argument of function I_0 with the help of identity (90), finally one obtains:

$$\int d^2x_{\rm T}\,\rho_P^{\rm in}(k,\boldsymbol{x}_{\rm T},0)$$

$$=\frac{2b}{k}\Theta\left(\frac{Q_0}{\theta}<k<P\right)\int\limits_{\frac{Q_0}{k}}^{\theta}\frac{d\theta_{Pk}}{\theta_{Pk}}I_0\left(\sqrt{8b\,\ln\left(\frac{P}{k}\right)\ln\left(\frac{k\theta_{Pk}}{Q_0}\right)}\right), \tag{99}$$

which equals the normalization of particle density in momentum space defined in (52):

$$\int d^2x_{\rm T}\ \rho_P^{\rm in}(k,\boldsymbol{x}_{\rm T},0)=\int d^2k_{\rm T}\ \rho_P^{\rm in}(k,\boldsymbol{k}_{\rm T}). \tag{100}$$

REFERENCES

[1] B. Ziaja, hep-ph 9705473.

[2] R. Hanbury-Brown, R.Q. Twiss, *Nature* (London) **177**, 27 (1956) .

[3] D.H. Boal, C.- K. Gelbke, B.K. Jennings, *Rev. Mod. Phys.* **62**, 553 (1990).

[4] W. Ochs, J. Wosiek, *Phys. Lett.* **B305**, 144 (1993); Y.U. Dokshitzer, I. Dremin, *Nucl. Phys.* **B402**, 139 (1993); P. Brax, J.-L. Meunier, R. Peschanski, *Z. Phys.* **C62**, 649 (1994); R. Peschanski, *Multiparticle Dynamics 1992*, World Scientific, Singapore 1993.

[5] Yu.L. Dokshitzer, V.A. Khoze, A.H. Mueller, S.I. Troyan, *Basics of Perturbative QCD*, Editions Frontiers, Gif-sur-Yvette Cedex, France, 1991 and references therein.

[6] Ya.I. Azimov, Yu.L. Dokshitzer, V.A. Khoze, S.I. Troyan, *Z. Phys.* **C27**, 65 (1985); *Z. Phys.* **C31**, 231 (1986).

[7] Yu.L. Dokshitzer, *Phys. Lett.* **B305**, 295 (1993) and references therein.

[8] J.-L. Meunier, R. Peschanski, INLN-96-01 and references therein.

[9] A. Bialas, M. Krzywicki, *Phys. Lett.* **B354**, 134 (1995).

[10] B. Ziaja, *Acta Phys. Pol.* **B27**, 2179 (1996).

[11] V.S. Fadin, *Yad. Fiz.* **37**, 408 (1983); Yu.L. Dokshitzer, V.S. Fadin, V.A. Khoze, *Z. Phys.* **C15**, 325 (1982); *Z. Phys.* **C18**, 37 (1983).

[12] J. Wosiek, *Acta Phys. Pol.* **B24**, 1027 (1993); W. Ochs, J. Wosiek, *Phys. Lett.* **B305**, 144 (1993) .

[13] P.M. Morse, H. Feshbach, *Methods of Theoretical Physics I*, McGraw-Hill Book Company, Inc. 1953, p.453.

[14] A.H. Mueller, *Nucl. Phys.* **B415**, 373 (1994) .

[15] J.D. Jackson, *Classical Electrodynamics*, J. Wiley & Sons 1975.